

Title:

An investigation of shock-accelerated, unstable gas cylinders using simultaneous density-field visualization and PIV

Author(s):

C. Tomkins, K. Prestridge, C. Zoldi, P. Rightley, P. Vorobieff and R. Benjamin

Submitted to:

<http://lib-www.lanl.gov/la-pubs/00796264.pdf>

An investigation of shock-accelerated, unstable gas cylinders using simultaneous density-field visualization and PIV.

C. Tomkins, K. Prestridge, C. Zoldi, P. Rightley, P. Vorobieff and R. Benjamin

Abstract

Simultaneous density and particle image velocimetry measurements are performed on a shock-accelerated, unstable cylinder of dense gas. Density-based instability growth estimates show good agreement with two-dimensional simulations by an adaptive-mesh Eulerian solver. However, a more rigorous comparison between the computational velocity field and the PIV data reveals significant differences between the fluctuating velocity magnitudes in the flowfields. Flow visualization results from a double-cylinder gas configuration, in which the unstable cylinders interact spanwise as they evolve, are also compared with a preliminary simulation.

1

Introduction

The Richtmyer-Meshkov instability (RMI) (Meshkov, 1969) occurs during the impulsive acceleration of a perturbed interface between two materials of different density; the misalignment of the density gradient and pressure gradient leads to a baroclinic production of vorticity. RMI plays an important role in several areas, ranging from inertial confinement fusion to the evolution of supernovae, but the complexity of the instability often makes the prediction of fundamental late-time behavior, such as the degree of mixing, difficult. In the present work, we perform an experimental and computational investigation of the pre-turbulent instability created by the interaction of a planar shock with a heavy-gas (SF_6) cylinder surrounded by air. Simultaneous planar density and velocity measurements are obtained (Prestridge *et al.*, 2000a), permitting a detailed, quantitative comparison with simulations for the first time. The principal results of this comparison are summarized in the present paper; for a more thorough description, the reader is referred to Prestridge *et al.* (2001).

2

Experimental and computational details

To create the cylinder, SF_6 gas driven by a gravity-feed system enters from the top of the test section through a circular nozzle. Glycol droplets that trace the dense gas are mixed with it *a priori*; analysis of the flow tracking fidelity and direct Rayleigh scattering measurements confirm that the particles follow the flow (Rightley *et al.*, 1999). The Mach 1.2 shock accelerates the cylinder to approximately 100 m/s, and its post-shock evolution is imaged at six distinct times, 140 μs apart, using a customized Nd:YAG laser spread into a sheet. An additional laser pulse is provided a short time after the sixth pulse, which allows for one PIV measurement per realization, imaged with an independent camera. An additional (third) camera is used to capture the initial density profile in two dimensions, immediately before the shock impact (Prestridge *et al.*, 2000b).

The instability is simulated using RAGE, a multidimensional Eulerian hydrodynamics code (Baltrusaitis *et al.*, 1996). RAGE is an inviscid code which allows for continuous adaptive mesh refinement. Zones are refined to follow gradients in the flowfield, such as shocks, contact discontinuities, and material interfaces. The experimental initial density profile is used as the initial condition for the simulation, so that any asymmetries in the cylinder are incorporated into the simulations. The cylinder evolution is computed in the "center of mass" frame, an approach that reduces the effects of numerical advection.

3

Summary of single-cylinder results

Figure 1 shows evolving density profiles for one experimental and one computational realization (Zoldi, 2001). The computational data are extracted at the same times as in the experiment. Inspection of the figure reveals quite good visual agreement between the two sets of results. The height and width of the structures are about 15-20% larger in the experiment than in the computations, and the onset of a secondary instability—a Kelvin-Helmholtz instability created by the shear between the heavy and light gas—appears at similar stages of development in both

C. Tomkins, K. Prestridge, P. Rightley, R. Benjamin. Dynamic Experimentation Division, Los Alamos National Laboratory, Los Alamos, NM, USA.

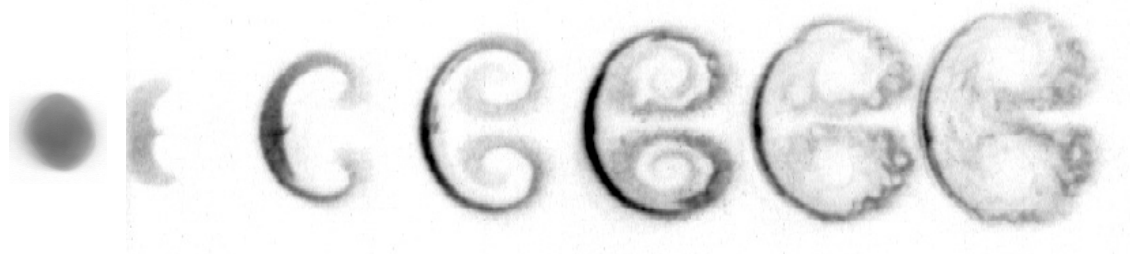
C. Zoldi. Applied Physics Division, Los Alamos National Laboratory, Los Alamos, NM, USA.

P. Vorobieff. Department of Mechanical Engineering, University of New Mexico, Albuquerque, NM, USA.

Correspondence to:

Dr. Christopher Tomkins, Dynamic Experimentation Division, MS D454, Los Alamos National Laboratory, Los Alamos, NM 87501 USA.

E-mail: ctomkins@lanl.gov



(a) Images of density fields of initial conditions ($t = 0$, immediately prior to shock impact) and at $t = 50, 190, 330, 470, 610, 750 \mu\text{s}$ after shock impact.



(b) Simulation of the experiment using image of initial conditions at $t = 0, 50, 190, 330, 470, 610, 750 \mu\text{s}$.

Figure 1. Experimental and computational density fields.

cases. Thus, traditional comparisons of integral lengths (often referred to as “mixing widths”) suggest the simulations are capturing the evolution with reasonable accuracy.

A more rigorous test, however, is provided by the PIV data. Figure 2 shows velocity vectors from both the experiment and computation at $t = 750 \mu\text{s}$ after shock impact. The vector plots are shown in a convective reference frame, in which the convective velocity is equal to the frame average velocity. These fields contain similar vector patterns, capturing most of a pair of counter-rotating vortices. Note, however, the difference in the magnitude of the vector scale between the two figures. The computations predict fluctuating velocities that are significantly larger than those observed in the experiment. This difference is quantified in Figure 3, which presents a histogram of the magnitudes of the fluctuating velocities (where the mean velocity is again the frame average velocity) for both experiment and simulation. The experimental data are confined to the range 0–12 m/s, while the range of most probable computational velocities extends from approximately 13 m/s to 35 m/s. Yet greater values of the fluctuating velocity magnitude are also populated by the simulated data in lesser, but not insignificant, quantities.

Additional comparisons of vorticity and total circulation are also performed; these show equally poor agreement. This difference suggests that the present flowfield is highly demanding computationally, and provides a rigorous test for code development, despite its apparent simplicity. We are currently investigating in greater detail the reasons for these differences.

4

Preliminary double-cylinder results

An additional set of measurements are performed with two dense-gas cylinders, separated in the spanwise direction, as the initial condition. All other conditions, including the incident shock, are unchanged from the single-cylinder experiment. The initial, center-to-center cylinder spacing, S , is varied from 1.2 to 2.0 times the cylinder diameter, D , in increments of $0.2D$ (schematically depicted in Figure 4). The evolution and interaction of the unstable cylinders is observed downstream after the shock has passed. Preliminary experimental data suggest that the resulting flow morphology is highly sensitive to the initial spacing. The two-cylinder problem provides a computational test that involves a relatively simple initial configuration, like the single-cylinder case, but the resulting flow exhibits even greater complexity, and greater sensitivity to initial conditions. Based on our experience with the single-cylinder results, we expect the forthcoming double-cylinder PIV experiments to provide essential data for rigorous, quantitative code validation.

Flow visualization data for the two-cylinder case are presented in Figure 5 for three values of the initial separation, S . An example of weak interaction is shown in Figure 5(a). In this case $S = 2.0D$, and the cylinders are qualitatively similar to two independently-evolving single cylinders. The effects of the interaction are evident,

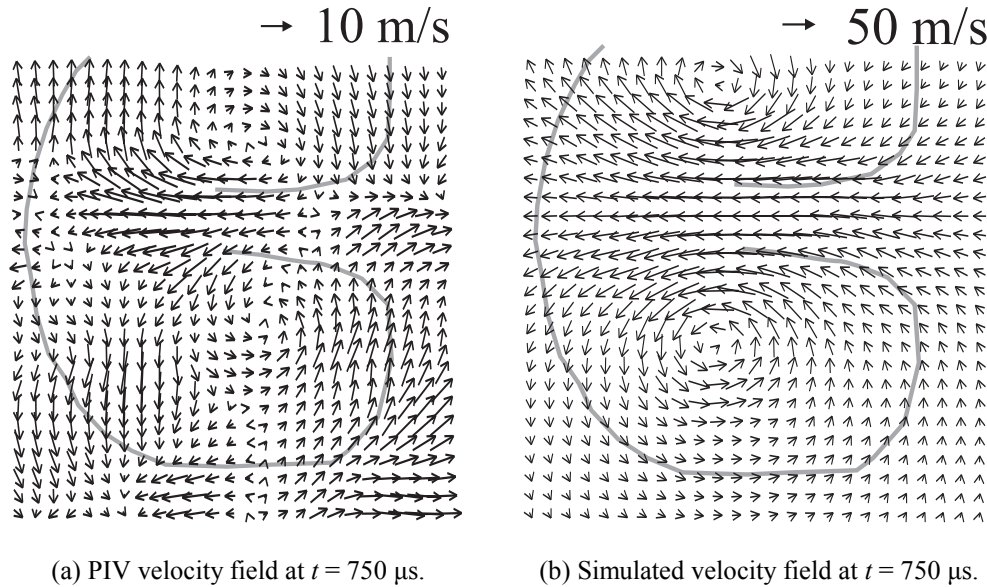


Figure 2. Experimental and computational velocity fields.

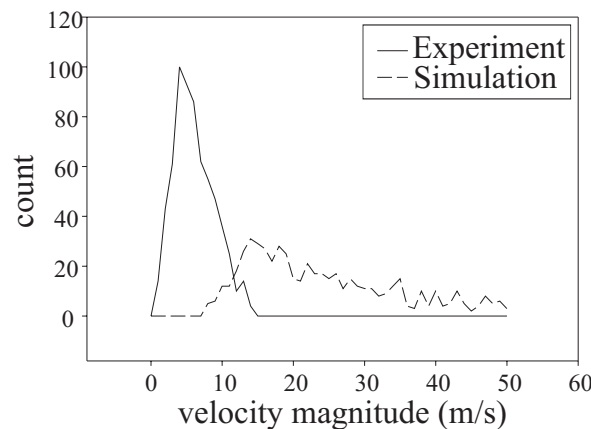


Figure 3. Histogram of magnitude of fluctuating velocity for both computation and experiment.

however: the individual structures are rotated in-plane relative to the single-cylinder case, and both inner vortices are slightly less developed than the outer vortices.

An example of “moderate” interaction is shown in Figure 5(b). Here the initial cylinder spacing is slightly smaller, $S = 1.6D$, and the resulting flow structures are significantly altered. The development of the innermost vortices is highly retarded, possibly due to vorticity cancellation shortly after the shock passage, or vortex interaction during the observed post-shock flow evolution. The proximity of the two cylinders may also have affected the initial shock–cylinder interaction, and hence affected the initial deposition of vorticity. A complete understanding of these issues, however, requires additional analysis, interpretation, and/or measurements.

The highest degree of interaction, labeled “strong” interaction, is evident in Figure 5(c). The nominal initial cylinder spacing is $S = 1.2D$, so that the spacing between the innermost edges of the cylinders is only $0.2D$. It is clear from the figure that the resulting flow structure bears a remarkable similarity to the single-cylinder structure, suggesting complete annihilation or cancellation of the innermost vortices. The effects of a secondary instability (Kelvin-Helmholtz) are also visible along the edges of the dense gas within the flow structures at later time—as in the single-cylinder data. A small gap in the density fields, located along the spanwise centerline of the image, serves as evidence that these were initially separate cylinders.

The foregoing results and interpretation, although preliminary, clearly reveal interesting and complex behavior, including a keen sensitivity of the cylinder–cylinder interaction and resulting flow morphology to the initial cylinder

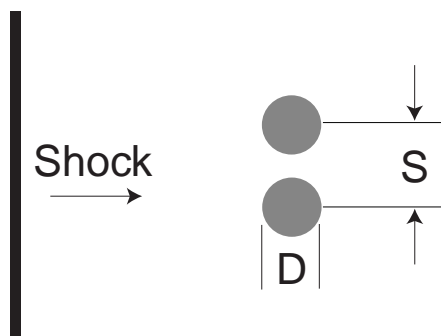
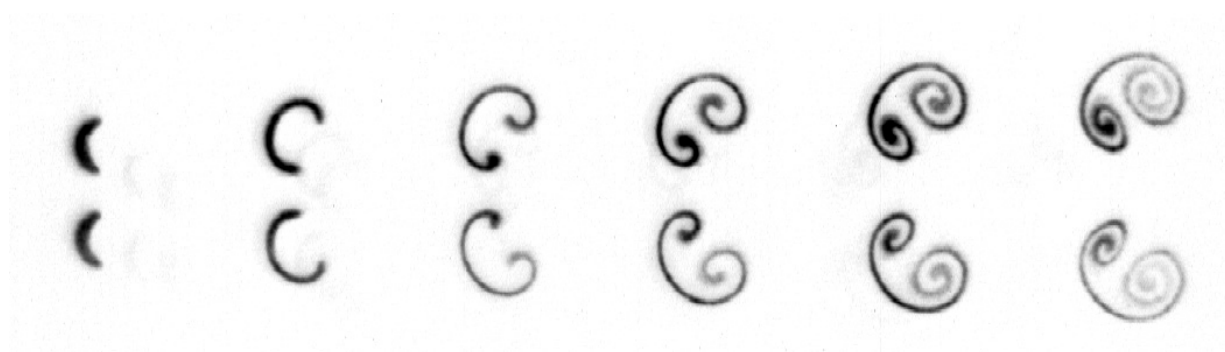
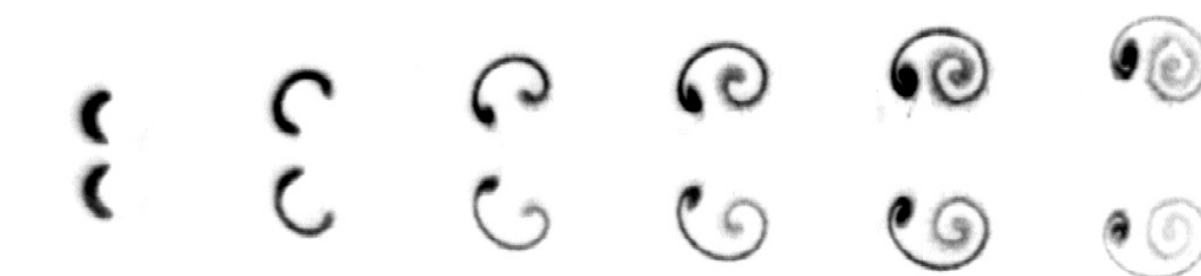


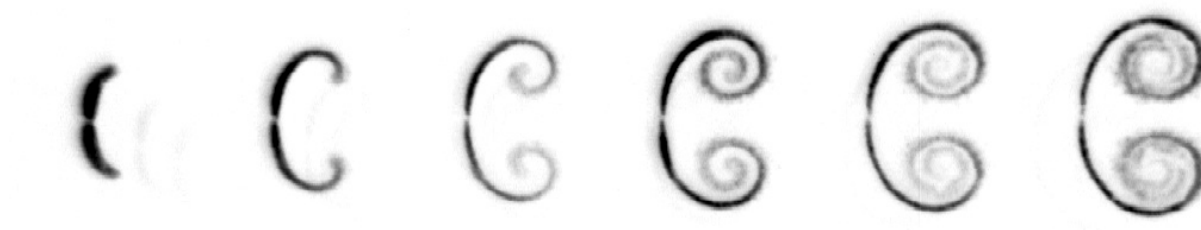
Figure 4. Top-view schematic of double-cylinder configuration with incident shock.



(a) Weak interaction. $S = 2.0D$.



(b) Moderate interaction. $S = 1.6D$.



(c) Strong interaction. $S = 1.2D$.

Figure 5. Density fields of two spanwise-interacting cylinders for three values of the initial cylinder spacing, S . Images acquired at $t = 50, 190, 330, 470, 610$, and $750 \mu s$ after shock impact.



Figure 6. Simulated density field of two spanwise-interacting cylinders for $S = 2.0D$. Data presented at $t = 50, 190, 330, 470, 610$, and $750 \mu\text{s}$ after shock impact.

separation. Additional analysis and interpretation is currently underway. Highly conclusive interpretation of the phenomenon, however, requires additional information about the flowfield—in particular, estimates of the velocity and vorticity fields. Current experimental efforts include PIV measurements at late time with the existing diagnostic system (Prestridge *et al.*, 2001). Current experimental improvements include seeding the surrounding air with particles, to improve the spatial resolution and the signal-to-noise ratio of the PIV measurements. Future experimental efforts will include PIV measurements at early time, which will allow us to investigate the accuracy of two important aspects of the computations: the estimate of initial baroclinic vorticity production, and the subsequent evolution of this deposited vorticity.

Preliminary simulations allow for qualitative comparison with experimental data for one case of the double-cylinder configuration, $S = 2.0D$. The initial conditions in this simulation are idealized, i.e. the cylinders are assumed to be perfectly circular in cross-section with sharp interfaces. The density field from this simulation is presented in Figure 6. Inspection of the images reveals that qualitative differences exist between the experiment, Figure 5(a), and the simulation. For example, the degree of interaction between the structures is clearly greater in the simulation, at both early and late time. Another interesting difference is in the induced motion of the vortices. In the simulation, the innermost vortices induce each other forward, so that they both move downstream, ahead of the outer structures. This motion is consistent with the motion of point vortices, of equal strength, in a plane. The experimental data, however, show that the innermost vortices lag the outer structures, for all separations studied. This motion is clearly inconsistent with the motion of idealized vortices of equal strength, but would be consistent with idealized vortex dynamics if the outer vortices were significantly stronger than the inner vortices. Clearly, this difference in behavior requires further investigation; however, this preliminary comparison suggests that there exist significant differences between the experimental and computational estimates of the vorticity field at early time, in particular the relative strengths of the inner and outer vortices. PIV measurements will be crucial in determining whether these differences are primarily associated with shock–cylinder interactions, or with post-shock vortex dynamics.

5 Conclusions

The evolution of Richtmyer–Meshkov-unstable gas cylinders has been studied experimentally and compared with computations. In the case of a single unstable cylinder, a comparison of density fields using traditional quantities, such as the instability growth rate, suggests that the computations adequately capture the relevant physics of the flow. However, a more rigorous test—a comparison of the fluctuating velocity fields—reveals that significant differences exist between the experiment and simulation, warranting further investigation.

The evolution and interaction of two unstable cylinders with spanwise separation is also investigated. Flow visualization data show that the degree of cylinder–cylinder interaction—and hence the resulting flow morphology—is highly sensitive to the initial cylinder separation. Fundamental differences are observed between the experimental and preliminary computational estimates of the density field for $S = 2.0D$. Additional PIV measurements (in progress) are required to fully understand the underlying reasons for these differences.

Acknowledgements

We acknowledge beneficial discussions with Michael Gittings, James Glimm and David Sharp, and the technical assistance of James Doyle, Norman Kurnit, and Michael Schneider. This work was supported by DOE contract W-7405-ENG-36 and by Sandia National Laboratories grant BG-7553.

References

- Baltrusaitis, R; Gittings, M; Weaver, R; Benjamin, R; Budzinski, J** (1996) Simulation of shock-generated instabilities. *Phys. Fluids*, Vol. 8, p. 2471.
- Meshkov, E** (1969) Instability of the interface of two gases accelerated by a shock wave. *Izv. Akad. Nauk. SSSR Mekh. Zhidk. Gaza.*, Vol 4, p. 151.
- Prestridge, K; Rightley, P; Vorobieff, P; Benjamin, R** (2000a) Simultaneous density-field visualization and PIV of a shock-accelerated gas curtain. *Exp. Fluids*, Vol. 29(4), p. 339.
- Prestridge, K; Vorobieff, P; Rightley, P; Benjamin, R** (2000b) Validation of an instability growth model using particle image velocimetry measurements. *Phys. Rev. Lett.*, Vol. 84, p. 4353.
- Prestridge, K; Zoldi, C; Vorobieff, P; Rightley, P; Benjamin, R** (2001) Experiments and simulations of instabilities in a shock-accelerated gas cylinder. Submitted to *Phys. Fluids*.
- Rightley, P; Vorobieff, P; Benjamin, R** (1999) Experimental observations of the mixing transition in a shock-accelerated gas curtain. *Phys. Fluids*, Vol. 11(1), p. 186.
- Zoldi, C.** (2001) A numerical and experimental study of a shock-accelerated heavy gas cylinder. Ph.D. Thesis, SUNY at Stony Brook.